FIRST EVIDENCE OF MULTIPLE OCTAHEDRAL Al SITES IN Na-MONTMORILLONITE BY ^{27}Al MULTIPLE QUANTUM MAS NMR

Takafumi Takahashi*, Koji Kanehashi, and Koji Saito

Advanced Technology Research Laboratories, Nippon Steel Corporation, 20-1 Shintomi, Futtsu, 293-8511 Japan

Abstract—The configuration of hydroxyl groups around the octahedral cations of 2:1 phyllosilicate minerals has long been an important question in clay science. In the present study, ^{27}Al multiple quantum (MQ) magic angle spinning nuclear magnetic resonance (MAS NMR) was applied to the local structural analysis of octahedral Al positions in a purified Na-montmorillonite. Three octahedral Al sites ($^{[6]}$Al$_a$, $^{[6]}$Al$_b$, and $^{[6]}$Al$_c$) are distinguished by ^{27}Al 5QMAS NMR, whereas these sites are not differentiated by ^{27}Al MAS and 3QMAS NMR. The isotropic chemical shift (δ_{cs}) and the quadrupolar product (P_Q) were estimated to be 5.8 ppm and 2.6 MHz for $^{[6]}$Al$_a$, 6.2 ppm and 3.0 MHz for $^{[6]}$Al$_b$, and 6.7 ppm and 3.7 MHz for $^{[6]}$Al$_c$, respectively. The three Al sites originated from geometric isomers with *cis* and *trans* structures, which have mutually different configurations of the OH groups around the central Al^{3+} ions. From the view point of symmetry for the OH groups, $^{[6]}$Al$_a$ and $^{[6]}$Al$_b$ in the upfield region were assigned to *cis* sites, and $^{[6]}$Al$_c$ in the downfield region was assigned to a *trans* site. The occurrence of multiple Al sites implies that Na-montmorillonite used in the present study has *cis*-vacant structure in the octahedral sheet. This is a reasonable insight, supported by the chemical composition and the differential thermal analysis data of the Na-montmorillonite.

Key Words—*Cis*, Hydroxyl, MQMAS NMR, Na-montmorillonite, Octahedral Al, *Trans*.

INTRODUCTION

Na-montmorillonite is one of the most useful of all layer silicates, and is used as a buffer material in the geological disposal of high-level radioactive wastes (Komine, 2004) and as a host material for clay-polymer nanocomposites (Xue and Pinnavaia, 2007). These uses are due to its properties such as low permeability (Benna *et al.*, 2001), swelling with absorption of water (Mooney *et al.*, 1952), high capacity for adsorption of cations (Abollino *et al.*, 2003), and alignment in magnetic fields (Koerner *et al.*, 2005; Takahashi *et al.*, 2006). To elucidate these properties and to optimize the applications, structural analysis of Na-montmorillonite at the molecular scale is required.

Drits *et al.* (2006) described 2:1 phyllosilicates as being *cis*-vacant (*cv*) or *trans*-vacant (*tv*) depending on the cation site occupancy. For Mg-rich montmorillonites with random distribution of octahedral cations, the *cv* structure better compensates the negative charge in the octahedral sheets than the *tv* structure because in the *cv* structure the negative charge located in two adjacent OH groups can be compensated by three octahedral cations (Drits *et al.*, 2006). Formation of *cv* and *tv* phyllosillicates is controlled by the composition and distribution of octahedral cations and by the degree of Si-Al substitution in tetrahedral sheets (Tsipursky and Drits, 1984; Cuadros, 2002; Drits *et* *al.*, 2006). Apart from the controlling factors for distribution of octahedral cations between *cis* and *trans* sites, *cis*- or *trans*-vacant structure is generated depending on the configuration of OH groups The configuration of OH groups certainly affects the local structure of the central octahedral cations. Investigating the local structure around the specific octahedral cation, therefore, provides information on OH-group configuration, and consequently leads to determination of the distribution of cations between *cis* and *trans* sites in the octahedral sheet of phyllosilicates.

Solid-state NMR is a powerful experimental approach for investigating the local structure of crystalline and non-crystalline materials. This is because solid-state NMR provides information on chemical environments around the specific nucleus. ^{29}Si and ^{27}Al MAS NMR have been applied to structural analysis of various phyllosilicates and zeolites (Lippmaa *et al.*, 1980, 1986; Fitzgerald *et al.*, 1995; Cong and Kirkpatrick, 1996). Although a ^{27}Al MAS NMR spectrum is often broadened due to the second-order quadrupolar interaction, multiple quantum MAS (MQMAS) NMR, proposed by Frydman and Harwood (1995), is a promising method which provides a high-resolution NMR spectrum by completely averaging the second-order quadrupolar interaction. ^{27}Al 3QMAS NMR, therefore, has been used to study the local structure in Na-montmorillonite (Ohkubo *et al.*, 2003), chlorite (Zazzi *et al.*, 2006), and other aluminosilicates (Gore *et al.*, 2002; Bardy *et al.*, 2007).

As shown by Zazzi *et al.* (2006), MQMAS NMR has the potential to distinguish geometric isomers of octahedral Al sites in phyllosilicates. The 3QMAS
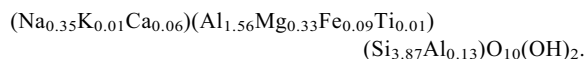
520

NMR spectrum for Na-montmorillonite, however, has shown one 6-coordinated Al ([6]Al) site (Ohkubo *et al.*, 2003; Takahashi *et al.*, 2007). This indicates that the resolution of 3QMAS NMR might be insufficient to distinguish the geometric isomers of octahedral Al in Na-motmorillonite. In this study, ^{27}Al 5QMAS NMR, generally providing greater resolution than 3QMAS, as well as conventional ^{27}Al MAS and ^{27}Al 3QMAS NMR, was applied to the structural analysis of purified Na-montmorillonite. Based on the results obtained by these analyses, insights were gained into the symmetry of the OH groups around octahedral Al^{3+} ions and the distribution of octahedral cations between *cis* and *trans* sites.

EXPERIMENTAL

Material

Kunipia-F montmorillonite, prepared by purifying the Tsukinuno montmorillonite (JCSS-3101), a standard material supplied by the Clay Science Society of Japan, was purchased from Kunimine Industry Co., Ltd. The chemical composition of Kunipia-F was determined by XRF analysis:

$$(Na_{0.35}K_{0.01}Ca_{0.06})(Al_{1.56}Mg_{0.33}Fe_{0.09}Ti_{0.01})$$
$$(Si_{3.87}Al_{0.13})O_{10}(OH)_2.$$

Kunipia-F was further purified by following the procedure of Sato (2005), because small amounts of impurities (<1%) such as carbonate minerals and quartz occur in the sample. The resultant sample (Kunipia-P) was analyzed by XRD to confirm the absence of quartz and other impurities. Kunipia-F and Kunipia-P differ only in terms of their impurities; their basic properties are indistinguishable. In this study, only Kunipia-P was used for solid-state NMR experiments in order to acquire Al signals from a pure Na-montmorillonite.

^{27}Al MAS and MQMAS NMR experiments

Kunipia-P was packed in a 4 mm zirconia (ZrO_2) rotor. ^{27}Al MAS and MQMAS NMR experiments were conducted using a JEOL ECA-700 (16.4 T) spectrometer with a CP/MAS probe.

^{27}Al MAS and MQMAS NMR spectra were obtained with a spinning rate of 18 kHz ± 3 Hz. A pulse repetition time of 0.3 s was applied to achieve full relaxation. A 1.0 M aqueous $AlCl_3$ solution was used as an external chemical shift reference (−0.1 ppm). In all experiments, the offset of chemical shift was set to 8.45 ppm.

The ^{27}Al MAS NMR spectrum was obtained by using π/6 single pulse excitation. In the [27]Al MQMAS experiments, a three-pulse sequence with z-filter (Figure 1) was used to selectively excite and convert 3Q or 5Q coherence. The excitation and conversion pulse lengths with the r.f. field of 12.5 kHz were optimized to be 3.2 and 1.0 μs, respectively, for ^{27}Al 3QMAS NMR, and 3.0 and 1.0 μs for [27]Al 5QMAS

NMR. The third soft-pulse length with the low r.f. field of 4.4 kHz was optimized to be 14 μs. The t_1 increments (55.56 μs) were synchronized with the spinning rate (18 kHz) to fold the spinning side bands into the main peak along the F1 dimension. A scan time of 8 h was necessary in order to obtain sufficient signals in the 3QMAS NMR experiment, while a scan time of 33 h was necessary for 5QMAS NMR. Second dimensional MQMAS spectra were obtained in parallel with the F2 dimension by shearing transformation.

RESULTS AND DISCUSSION

^{27}Al MAS and 3QMAS NMR experiments

In a ^{27}Al MAS NMR spectrum (Figure 2), one 6-coordinated Al ([6]Al) site and one 4-coordinated Al ([4]Al) site are recognized. These sites correspond to octahedral and tetrahedral Al, respectively. This result is consistent with the data previously obtained under different experimental conditions (Ohkubo *et al.*, 2003; Takahashi *et al.*, 2007).

To investigate the local structure around octahedral Al^{3+} ions, an ^{27}Al 3QMAS NMR spectrum focused on the [6]Al sites was obtained. The [27]Al 3QMAS spectrum (Figure 3) shows one peak maximum with a tail along QIS. From the 3QMAS NMR spectrum, the isotropic chemical shift (δ_{cs}) and quadrupolar products (P_Q) were estimated using equations 1 and 2 (Amoureux *et al.*, 2002)

$$\delta_{cs} = \frac{10}{27}\delta_{MAS} + \frac{17}{27}\delta_{ISO} \qquad (1)$$

$$P_Q = \sqrt{\frac{170}{81}\frac{\left(4S(2S-1)\right)^2}{\left(4S(S+1)-3\right)}(\delta_{MAS}-\delta_{ISO})}\frac{v_0}{10^3} \qquad (2)$$
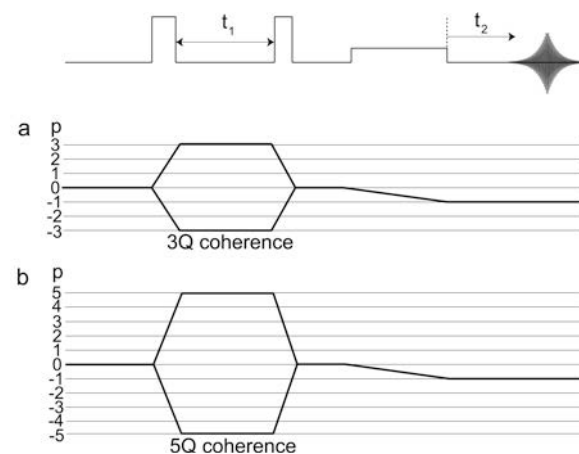

Figure 1. Pulse sequences with z-filter used for MQMAS NMR experiments. Coherence transfer pathways in (a) 3QMAS and (b) 5QMAS NMR experiments are also shown.
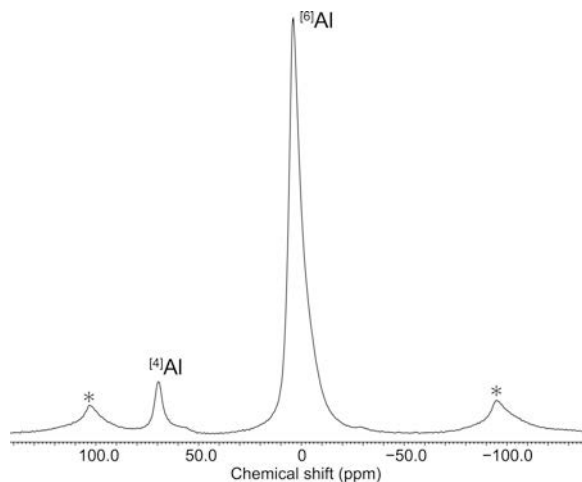
Figure 2. ^{27}Al MAS NMR spectrum of Kunipia-P obtained at 18 kHz and 100 scans. * indicates spinning side bands.
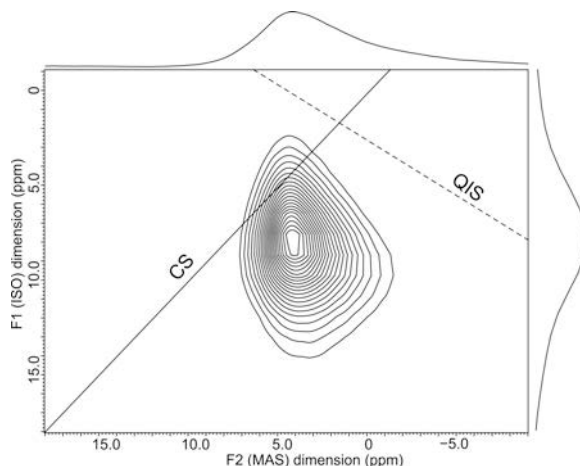

Figure 3. ^{27}Al 3QMAS spectrum of Kunipia-P obtained with a total of 16 t_1 points and 2880 scans for each point. The solid line labeled as CS indicates the chemical shift, whereas the dotted line labeled as QIS indicates the quadrupolar-induced shift.

Where S is the spin quantum number, and ν_0 the Larmor frequency for ^{27}Al. δ_{ISO} and δ_{MAS} are the positions (in ppm) for centers of gravity of peaks projected onto the F1(ISO) and F2(MAS) axes, respectively. The estimated δ_{cs} (6.6 ppm) and P_Q (3.6 MHz) values (Table 1) were reasonably consistent with previously determined values (Takahashi *et al.*, 2007). The observation of a single $^{[6]}$Al site means either that the OH groups around octahedral Al^{3+} ions show only one configuration, or that multiple Al sites with different structure such as *cis* and *trans* configurations cannot be distinguished by 3QMAS NMR.

To examine these possibilities, a ^{27}Al 5QMAS NMR experiment focusing on the $^{[6]}$Al sites was performed. The ^{27}Al 5QMAS NMR spectrum (Figure 4) indicates that the resolution of 5QMAS is greater than that of 3QMAS, although the sensitivity is less. In the 5QMAS spectrum, at least three $^{[6]}$Al sites ($^{[6]}$Al$_a$, $^{[6]}$Al$_b$, and $^{[6]}$Al$_c$) were observed. The δ_{cs} and P_Q values for all $^{[6]}$Al sites were estimated from the peak maximum of each site using equations 1 and 2 (Table 1).

The chemical shift in NMR reflects the electronic structure around the observed nucleus. The electronic structure varies depending not only on coordination number and ligand type, but also on three-dimensional symmetry, although the latter effect on the electronic structure is often smaller than the former. For polyhedral

structures with the same coordination number and the ligand type, but with non-equivalent symmetry of ligands, different chemical shifts are expected. In fact, multinuclear NMR spectroscopy focusing on central cations of the isomeric metal complexes show different chemical shifts depending on the symmetry of coordinating ligands (Yamasaki *et al.*, 1968; Brevard and Granger, 1983; Rochon and Buculei, 2004).

Although the studies described above deal with the geometric isomers of metal complexes dissolved in a solvent, an analogous discussion for octahedral Al in phyllosillicates was given by Zazzi *et al*. (2006). They applied ^{27}Al 3QMAS NMR to the structural analysis of synthetic chlorite and indicated that two of four octahedral Al sites were observed separately. Although
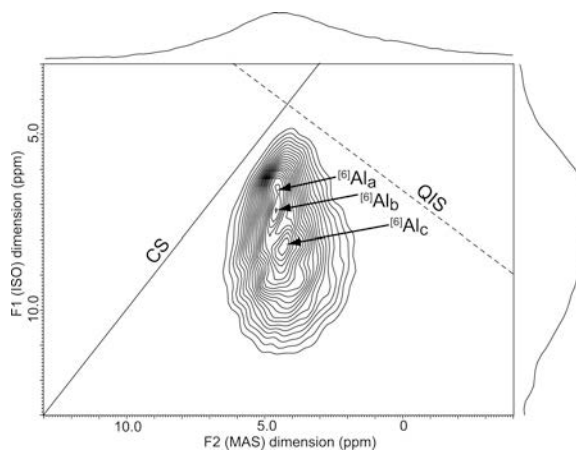
Table 1. Summary of isotropic chemical shifts (δ_{cs}) and quadrupolar products (P_Q) for each Al site observed in ^{27}Al 3QMAS and 5QMAS NMR spectra.

	3QMAS $^{[6]}$Al	5QMAS $^{[6]}$Al$_a$	5QMAS $^{[6]}$Al$_b$	5QMAS $^{[6]}$Al$_c$
δ_{cs} (ppm)	6.5	5.8	6.2	6.7
P_Q (MHz)	3.6	2.6	3.0	3.7

Figure 4. ^{27}Al 5QMAS NMR spectrum of Kunipia-P obtained with a total of 16 t_1 points and 12,000 scans for each point. The solid line labeled as CS indicates chemical shift, while the dotted line labeled as QIS indicates the quadrupolar-induced shift.

their result indicated that 3QMAS NMR has insufficient resolution to identify *cis* and *trans* sites, ^{27}Al MQMAS NMR in principle can distinguish *cis* and *trans* sites in phyllosillicates. Assignments of the multiple Al sites in the 5QMAS NMR spectrum, therefore, were considered from the view point of symmetry for OH groups coordinating octahedral Al^{3+} ions.

The octahedral cation sites are classified into three types according to the symmetry of coordinating OH groups; one *trans* (M_1) and two *cis* sites (M_2, M_2'). Cations are not actually positioned in vacant M_2' sites. This means that occupied octahedral Al positions ideally consist of two (M_1 and M_2) sites. The number of multiple Al sites identified in the 5QMAS NMR spectrum of Kunipia-P is, therefore, inconsistent with the ideal. Both Al_a and Al_b are, however, observed quite close together in the 5QMAS spectrum. This indicates that Al_a and Al_b are basically ascribed to the octahedral Al position with the same OH configuration, but have slightly different structures because of the slight distortion in local symmetry of the nearest ligands (OH groups and O atoms).

Such a small distortion in the local symmetry is probably generated by a particular distribution of cations in a second neighbor. Substitution of Al for tetrahedral Si can generate a small distortion in local symmetry. As a result of Al substitution in the tetrahedral cation site, the electronic structure of an oxygen atom shared by the substituted tetrahedron and an adjacent octahedron would be changed, or an oxygen atom with the localized negative charge might interact with OH groups nearby to affect coordination of the OH groups to octahedral cations. These mechanisms might lead to the change in local chemical environments in the position of octahedral cations. Because the distortion in local symmetry of the nearest ligands adds a small perturbation to the chemical coordination environments of central cations, the effect is not always observed in the NMR spectrum, *e.g.* in the case of Al_a and Al_b. The observation of a single site (Al_c) in the downfield region is, therefore, reasonable, although Al_c should also be exposed to the same kind of local structural distortion. In addition, such a small structural perturbation caused by distortion in local ligand symmetry cannot explain the obvious distinction between [6]Al_a (or [6]Al_b) and Al_c. The explicit change in chemical shift is caused by a fundamental difference in ligand symmetry such as *cis* and *trans* configurations of OH groups in octahedral Al positions. The three [6]Al sites observed in the 5QMAS NMR spectrum are, therefore, assigned either to two *cis* and one *trans* sites, or to one *cis* and two *trans* sites.

Assignment of the three octahedral Al sites to the corresponding isomeric structure in octahedral sheets is not straightforward, but was, nevertheless, attempted taking into account previous studies of geometric isomers of metal complexes. The [103]Rh NMR spectroscopy of 6-coordinated Rh complexes, $[RhL_4(X)_2]^+$ (L =

PMe_3 or $AsMe_3$, X = Cl or Br), indicates that the chemical shift of *trans*-type coordination produces a downfield shift compared with *cis* complexes (Mann, 1991). The same relationship in chemical shifts of geometric isomers is known in the [59]Co NMR spectrum of $(Co(X)_4(Y)_2)$ complexes (Yamasaki *et al.*, 1968; Juranić *et al.*, 1977) and in the [99]Ru NMR spectra of Ru(bpy)(1-(2-pyridyl)-3,5-dimethylpyrazole)$_2$(PF)$_6$ complexes (Brevard and Granger, 1983; Steel *et al.*, 1983). The model calculation for $Co(X_4Y_2)$ complexes also indicates that the chemical shift for the *trans* CoX_4Y_2 (D_{4h}) structure generally shows a downfield shift with respect to the *cis* structure (Laszlo, 1983). The [6]Al_a and [6]Al_b observed in the upfield region are, therefore, assigned to *cis* sites, and [6]Al_c, observed in the downfield region, assigned to a *trans* site.

Although this assignment must be examined carefully, observation of the multiple octahedral Al sites requires a discussion of the vacant structure in the dioctahedral sheet. If the octahedral sheet of Kunipia-P has a *tv* structure, only the *cis* configuration of OH groups around the central Al^{3+} ions is allowed (Figure 5a). The *tv* structure model means that only one site should be observed even in the ^{27}Al 5QMAS NMR spectrum. This is not consistent with the results in the present study.

Multiple configurations of OH groups such as *cis* and *trans* sites are allowed when the octahedral sheet shows *cv* structure (Figure 5b). The *cv* structure model can, therefore, explain the multiple [6]Al sites observed by ^{27}Al 5QMAS NMR. The observation of multiple octahedral Al sites, hence, implies that Kunipia-P has *cv* structure in the octahedral sheet. Drits *et al.* (2006) stated that most Mg-rich montmorillonites have a *cv* structure if the distribution of octahedral cations is random, because the *cv* structure can more easily compensate the negative charges of OH groups than the *tv* structure by sharing two adjacent OH groups among three octahedral cations. From the chemical composition reported by Takahashi *et al.* (2007), Kunipia-P is certainly classified as a Mg-rich montmorillonite. The insight that Kunipia-P has a *cv* structure is, therefore, reasonable even in terms of chemical composition.

In addition, the differential thermal analysis (DTA) of *cv* 2:1 phyllosilicates are known to show an endothermic dehydroxylation peak at a greater temperature (650−800ºC) than *tv* phyllosilicates (500−600ºC) (Drits *et al.*, 1995). The DTA data of the unpurified montmorillonite (Tsukinuno montmorillonite) and Kunipia-F also show an endothermic point at the higher temperature (680−750ºC) (Uno *et al.*, 1992; Hedley *et al.*, 2007). The transformation of *cis*- and *trans*-vacant structures cannot occur during the preparation of Kunipia-P, because the purification process was performed at no more than 150ºC which is much less than the dehydroxylation temperature. Furthermore, exchangeable cation sites in the interlayer of
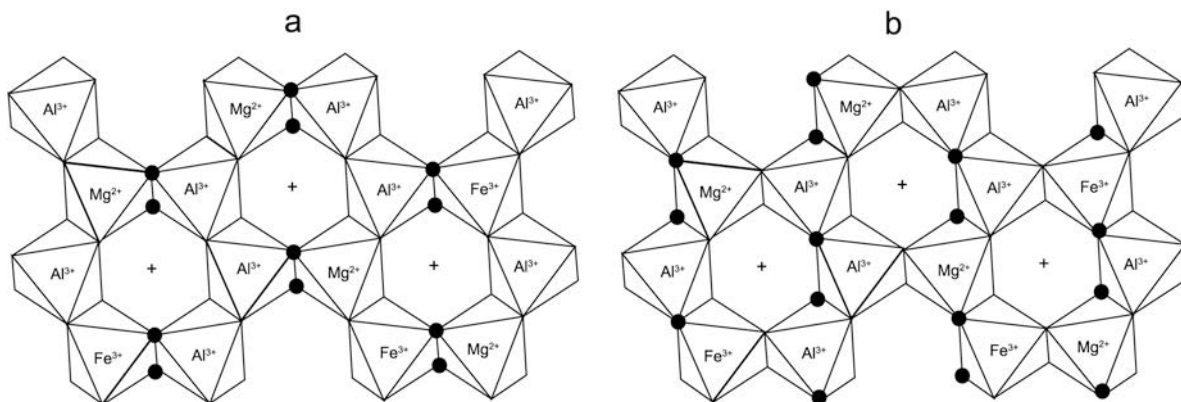
Figure 5. Schematic explanation of (a) *tv* and (b) *cv* structures for the dioctahedral phyllosilicates. Kunipia-P is proposed to have a *cv* octahedral structure. Distribution of Fe^{3+} and Mg^{2+} ions is assumed to be random. Filled circles (●) indicate OH groups.

the three samples (Tsukinuno montmorillonite, Kunipia-F, and Kunipia-P) are dominated by the Na^+ ion. The endothermic peak corresponding to dehydroxylation of Kunipia-P should, therefore, be identical to that of Kunipia-F or Tsukinuno-montmorillonite. This leads to an acceptable consequence that Kunipia-P used in the present study also shows dehydroxylation at high temperatures (680−750ºC), which is an important feature of montmorillonite with *cis*-vacant structure. The thermal analysis, therefore, also supports the assertion that Kunipia-P has a *cis*-vacant structure in its octahedral sheets.

CONCLUSIONS

MQMAS NMR techniques were applied to the structural analysis of octahedral Al sites in the purified Na-montmorillonite (Kunipia-P). A single octahedral Al site was observed by ^{27}Al MAS and 3QMAS NMR, while multiple octahedral Al sites were distinguished by ^{27}Al 5QMAS NMR. These multiple Al sites were interpreted to reveal a difference in symmetry of oxygen atoms and hydroxyl groups around octahedral Al^{3+} ions. Two sites in the upfield region were assigned to *cis* sites, while the other one in, the downfield region, was assigned to a *trans* site. The observation of multiple octahedral Al sites indicates that the purified montmorillonite (Kunipia-P) has a *cis*-vacant octahedral structure. This conclusion was also consistent with chemical and differential thermal analyses.

ACKNOWLEDGMENTS

REFERENCES

Abollino, O., Aceto, M., Malandrino, M., Sarzanini, C., and Mentasti, E. (2003) Adsorption of heavy metals on Na-montmorillonite. Effect of pH and organic substances. *Water Research*, **37**, 1619−1627.

Amoureux, J.P., Huguenerd, C., Engelke, F., and Taulelle, F. (2002) Unified representation of MQMAS and STMAS NMR of half-integer quadrupolar nuclei. *Chemical Physics Letters*, **356**, 497−504.

Bardy, M., Bonhomme, C., Fritsch, E., Maquet, J., Hajjar, R., Allard, T., Derenne, S., and Calas, G. (2007) Al speciation in tropical podzols of the upper Amazon Basin: A solid-state ^{27}Al MAS and MQMAS NMR study. *Geochimica et Cosmochimica Acta*, **71**, 3211−3222.

Benna, M., Kbir-Ariguib, N., Clinard, C., and Bergaya, F. (2001) Static filtration of purified sodium bentonite clay suspensions. Effect of clay content. *Applied Clay Science*, **19**, 103−120.

Brevard, C. and Granger, P. (1983) Ruthenium NMR spectroscopy: a promising structural and analytical tool. General trends and applicability to organometallic and inorganic chemistry. *Inorganic Chemistry*, **22**, 532−535.

Cong, X. and Kirkpatrick, R.J. (1996) ^{29}Si MAS NMR Study of the Structure of Calcium Silicate Hydrate. *Advanced Cement Based Materials*, **3**, 144−156.

Cuadros, J. (2002) Structural insights from the study of Cs-exchanged smectites submitted to wetting-and-drying cycles. *Clay Minerals*, **37**, 473−486.

Drits, V.A., Besson, G., and Mueller, F. (1995) An improved model for structural transformation of heat-treated aluminous dioctahedral 2:1 layer silicates. *Clays and Clay Minerals*, **43**, 718−731.

Drits, V.A., McCarty, D.K., and Zviagina, B.B. (2006) Crystal-chemical factors responsible for the distribution of octahedral cations over *trans* and *cis* sites in dioctahedral 2:1 layer silicates. *Clays and Clay Minerals*, **54**, 131−152.

Fitzgerald, J.J., Hamza, A.I., Bronnimann, C.E., and Dec, S.F. (1995) Studies of the solid/solution 'interfacial' delamination of kaolinite in HCL(aq) using ^{1}H CRAMPS and SP/MAS ^{29}Si NMR spectroscopy. *Journal of the American Chemical Society*, **119**, 7105−7113.

Frydman, L. and Harwood, J.S. (1995) Isotropic spectra of half-integer quadrupolar spins from bidimensional magic-angle spinning NMR. *Journal of the American Chemical Society*, **117**, 5367−5368.

Gore, K.U., Abraham, A., Hegde, H., Kumar, R., Amoureux, J.P., and Ganapathy, S. (2002) ^{29}Si, and ^{27}Al MAS/3Q-MAS NMR Studies of High Silica USY Zeolites. *Journal of Physical Chemistry B*, **106**, 6115−6120.

Hedley, C.B., Yuan, G., and Theng, B.K.G. (2007) Thermal analysis of montmorillonites modified with quaternary phosphonium and ammonium surfactants. *Applied Clay Science*, **35**, 180−188.

Juranić, N., Ćelap, M.B., Vućelić, D., Malinar, M.J., and Radivoja, P.N. (1977) The ^{13}C and ^{59}Co nuclear magnetic resonance study of mixed Co(III) complexes containing glycinato ligand. *Inorganica Chimica Acta*, **25**, 229−232.

Koerner, H., Hampton, E., Dean, D., Turgut, Z., Drummy, L., Mirau, P., and Vaia, R. (2005) Generating triaxial reinforced epoxy/montmorillonite nanocomposites with uniaxial magnetic fields. *Chemistry of Materials*, **17**, 1990−1996.

Komine, H. (2004) Simplified evaluation of swelling characteristics of bentonites. *Engineering Geology*, **71**, 265−279.

Laszlo, P. (editor) (1983) *NMR of Newly Accessible Nuclei*. chapter 9. Vol, **2**. Academic Press, London.

Lippmaa, E., Mägi, M., Samson, A., Engelhardt, G., and Grimmer, A.R. (1980) Structural studies of silicates by solid-state high-resolution silicon-29 NMR. *Journal of the American Chemical Society*, **102**, 4889−4803.

Lippmaa, E., Samson, A., and Magi, M. (1986) High-resolution aluminum-27 NMR of aluminosilicates. *Journal of the American Chemical Society*, **108**, 1730−1735.

Mann, B.E. (1991) *Transition Metal NMR*. Elsevier, New York, 177 pp.

Mooney, R.W., Keenan, A.G., and Wood, L.A. (1952) Adsorption of water vapor by montmorillonite. II. Effect of exchangeable ions and lattice swelling as measured by X-ray diffraction. *Journal of the American Chemical Society*, **74**, 1271−1374.

Ohkubo, T., Kanehashi, K., Saito, K., and Ikeda, Y. (2003) Observation of two 4-coordinated Al sites in montmorillonite using high magnetic field strength ^{27}Al MQMAS NMR. *Clays and Clay Minerals*, **51**, 513−518.

Rochon, R.D., and Buculei, V. (2004) Multinuclear NMR study and crystal structure of complexes of the types cis and trans-Pt(amine)$_2$I$_2$. *Inorganica Chimica Acta*, **357**, 2218−2230.

Sato, H. (2005) Effects of the orientation of smectite particles and ionic strength on diffusion and activation enthalpies of I$^-$ and Cs$^+$ ions in compacted smectite. *Applied Clay Science*, **29**, 267−281.

Steel, P.J., Ahousse, F.L., Lerner, D., and Marzin, C. (1983) New ruthenium(II) complexes with pyridylpyrazole ligands. Photosubstitution and ^{1}H, ^{13}C, and ^{99}Ru NMR structural studies. *Inorganic Chemistry*, **22**, 1488−1493.

Takahashi, T., Ohkubo, T., and Ikeda, Y. (2006) Montmorillonite alignment induced by magnetic field: Evidence based on the diffusion anisotropy of water molecules. *Journal of Colloid and Interface Science*, **299**, 198−203.

Takahashi, T., Ohkubo, T., Suzuki, K., and Ikeda, Y. (2007) High resolution solid state NMR study on dissolution and alteration of Na-montmorillonite under highly alkaline conditions. *Microporous and Mesoporous Materials*, **106**, 284−297.

Tsipursky, S.I. and Drits, V.A. (1984) The distribution of octahedral cations in the 2:1 layers of dioctahedral smectites. *Clay Minerals*, **19**, 177−193.

Uno, Y., Sasaki, T., and Tatematsu T. (1992) Dehydration process of smectites under controlled steam pressure. *Nendo Kagaku*, **32**, 129−138.

Xue, S. and Pinnavaia, T.J. (2007) Overview of clay-based polymer nanocomposites (CPN): Pp. 1−24 in: *Clay-based Polymer Nanocomposites (CPN)* (K.A. Carrado and F. Bergaya editors). CMS Workshop Lectures, The Clay Minerals Society, Chantilly, VA, USA.

Yamasaki, A., Yajima, F., and Fujiwara, S. (1968) Nuclear magnetic resonance studies on cobalt complexes. I. Cobalt-59 nuclear-magnetic resonance spectra of cobalt (III) complexes. *Inorganica Chimica Acta*, **2**, 39−42.

Zazzi, Å., Hirsch, T.K., Lenova, E., Kaikkonen, A., Grins, J., Annersten, H., and Eden, M. (2006) Structural investigations of natural and synthetic chlorite minerals by X-ray diffraction, Mössbauer spectroscopy and solid-state nuclear magnetic resonance. *Clays and Clay Minerals*, **54**, 252−265.